Mechanical behaviour of cadmium-boron and cadmium-tungsten particulate composites

SHU-EN HSU
Materials Science Section, Chung Shan Institute of Science and Technology, Lung-Tan, Taiwan

G. R. EDWARDS
Department of Mechnical Engineering, Naval Post-graduate School, Monterey, California, USA

J. C. SHYNE, O. D. SHERBY
Department of Materials Science and Engineering, Stanford University, Stanford, California, USA

Mechanical behaviour of particulate composites of cadmium containing 0.6 to 3 μm size particles of boron and tungsten (up to 30 vol %) were studied from −196 to 260° C (0.13 to 0.9 T_m). The marked strengthening of cadmium by the presence of fine particles is attributed to significant grain size and texture strengthening effects as well as to dispersion hardening effects.

1. Introduction

This investigation centres on the mechanical behaviour of cadmium containing large volume fractions of boron or tungsten particles. We were motivated in this effort not only by curiosity, but also by technological practicality, for cadmium-based composites have some potential of becoming useful engineering materials for the nuclear reactor industry. Cadmium alloys have always been common choices by the reactor industry for control rods; it is of historical interest to note that the very first nuclear reaction was controlled by the use of cadmium [1]. Particulate composites based on boron–cadmium alloys could be particularly interesting as potential nuclear materials, for both components have very good ability to take neutrons away from the nuclear chain reaction. Their control effectiveness is different, however. Cadmium has an excellent thermal cross-section (2550 barn) but does not absorb well over a spectrum of neutron energies. Thus, while cadmium is an effective control rod for the normal thermal power reactor, it is not desirable for use in epithermal reactors. Boron, on the other hand, is capable of absorbing neutrons over a very wide range of energies, but is susceptible to severe radiation damage, a problem which can potentially be minimized by dispersing relatively large boron particles in a ductile matrix [2].

In addition to cadmium–boron composites we also studied cadmium-tungsten composites. The latter were chosen because earlier studies revealed that tungsten particles ductilized zinc at room temperature and contributed to dispersion hardening at high temperatures [3–6].

2. Materials and experimental procedure

We prepared test specimens by a powder metallurgy process, previously reported in detail [3, 4, 6], utilizing a series of warm rollings and extrusions near the cadmium melting temperature, and producing a 7 mm rod as the end product. The initial metal powders were pure, as evidenced by the spectrographic analysis of Table I. Cadmium–boron and cadmium–tungsten composites, containing up to 30 vol% second phase, were com-

TABLE I Spectrographic analysis of as-received powders

Elements	Powders (ppm)		
	Cadmium*	Tungsten†	Boron‡
Al	–	6	5–10
Ca	–	34	5–20
Cr	–	13	1–15
Cu	30	3	0.5–2
Fe	–	81	20–50
Mg	–	6	50–150
Mn	–	6	1–5
Mo	–	130	–
Ni	–	7	1–5
Pb	100	–	5–10
Si	–	9	5–10
Sn	–	6	–
Tl	4	–	–

* Analysed by the Electronic Space Products, Inc, Los Angeles, California.
† Analysed by the General Electric Company, Cleveland, Ohio.
‡ Analysed by the United Mineral & Chemical Corp, New York, N.Y.

pared for their mechanical characteristics with as-cast cadmium (99.98% Cd), as-sintered cadmium, and powder metallurgy cadmium, i.e. cadmium powder subjected to the identical mechanical comminution used for preparing composites (designated as PMMC Cd).

Mechanical testing was done by compressing right circular cylinders (5.1 mm diameter and 7.6 mm long) in an Instron machine. Elevated temperature tests were performed in air. The few tensile samples tested were machined to have threaded grips and a gauge section 3.2 mm diameter and 15.8 mm long. Microstructural analysis by optical and scanning electron microscopy was used to approximate the average grain diameters and dispersed particle diameters reported in Table II. Calculated mean particle spacing reported in Table II represents the surface-to-surface distance between a particle and its nearest neighbour in a random three-dimensional array [8, 9].

3. Results

Optical photomicrographs of several of the materials reported herein are shown in Fig. 1. Two important features of the comminuted microstructures are immediately obvious. First, the powder metallurgy process produces a very fine grain structure, even without deliberate additions of dispersed particles (Fig. 1b). Second, our powder metallurgy mechanical comminutive process does indeed produce a very homogeneous distribution of dispersed particles (Fig. 1c).

Fig. 2 presents the stress–strain behaviour, at ambient temperature and initial strain-rate, $\dot{\epsilon}_0 = 2.7 \times 10^{-3}\ \text{sec}^{-1}$, of as-cast cadmium, as-sintered cadmium, powder metallurgy cadmium and three B–Cd composites. The results shown in this figure

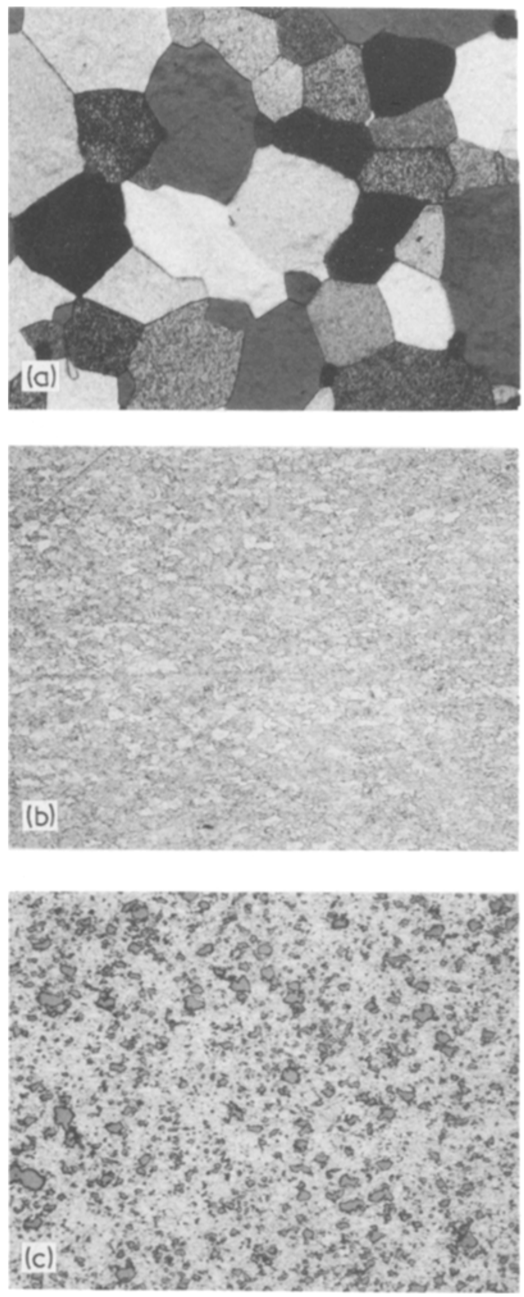

Figure 1 Microstructures of (a) as-cast cadmium (polarized light) × 75, (b) powder metallurgy cadmium, × 150. (c) 15 vol% boron-cadmium, × 150.

TABLE II Microstructural parameters of cadmium and cadmium-based composites

Material	Cadmium		Cadmium–boron			Cadmium–tungsten		
	As-cast	PMMC	3 (vol %)	15	30	1.4 (vol %)	15	30
Average particle diameter (μm)	–	30 (initial powder)	3	3	3	0.6	0.6	0.6
Average particle diameter (μm)	150	9	8	7.5	5 (est.)	–	–	–
Average particle spacing (μm)	–	–	49.4	7.5	2.2	36.4	2.5	0.7

emphatically demonstrate the importance of processing variables and composition on the mechanical behaviour of cadmium at ambient temperature.

Figs. 3 and 4 illustrate the influence of temperature, from 0.14 to $0.9T_m$, on the flow stress of cadmium–boron composites and cadmium–tungsten composites, respectively. As can be seen, the composites exhibit high strengths at all temperatures in comparison with as-cast cadmium.

4. Discussion

Several prominent features, found to be characteristic of cadmium and cadmium based composites when deformed at ambient temperature or below (0.13 to $0.5T_m$), are illustrated in Fig. 2. These mechanical characteristics are: (1) a significantly higher flow stress for powder metallurgy cadmium than for the more typical cast metal, (2) significant dispersion strengthening of the cadmium matrix for strains of about 10% with very little dispersion strengthening manifested at high strains, and (3) prominent strain-softening for all powder metallurgy alloys. In attempting to understand these observations it became clear that several important strengthening mechanisms contributed to the results obtained. Among these are grain size, texture strengthening, and dispersion hardening. We consider each of these contributions to the strength of cadmium and cadmium-based composites in the following sections.

5.1. Grain size strengthening

The mechanically processed powder metallurgy cadmium is considerably stronger than the as-cast cadmium at all temperatures (Fig. 2 and 3). Inasmuch as the powder metallurgy cadmium is fine grained, (9 μm), and the as-cast cadmium is coarse grained (150 μm) (Fig. 1a and 1b) it is tempting to attribute a major portion of the strength difference to a grain-size effect. Our studies, however, revealed that a strong $\langle 1 0 \bar{1} 0\rangle$ fibre texture, as in-

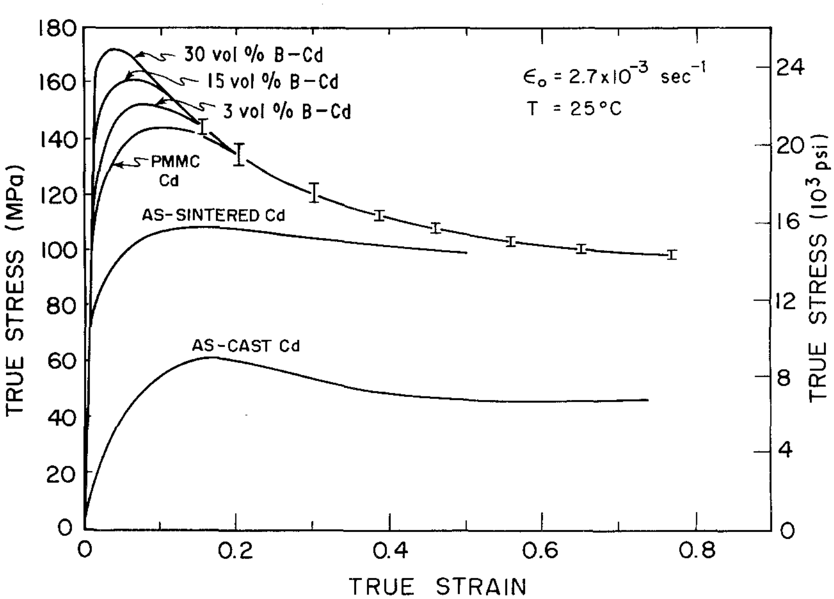

Figure 2 Compression true stress–true strain curves for as-cast cadmium, powder metallurgy processed cadmium and cadmium–boron particle composites.

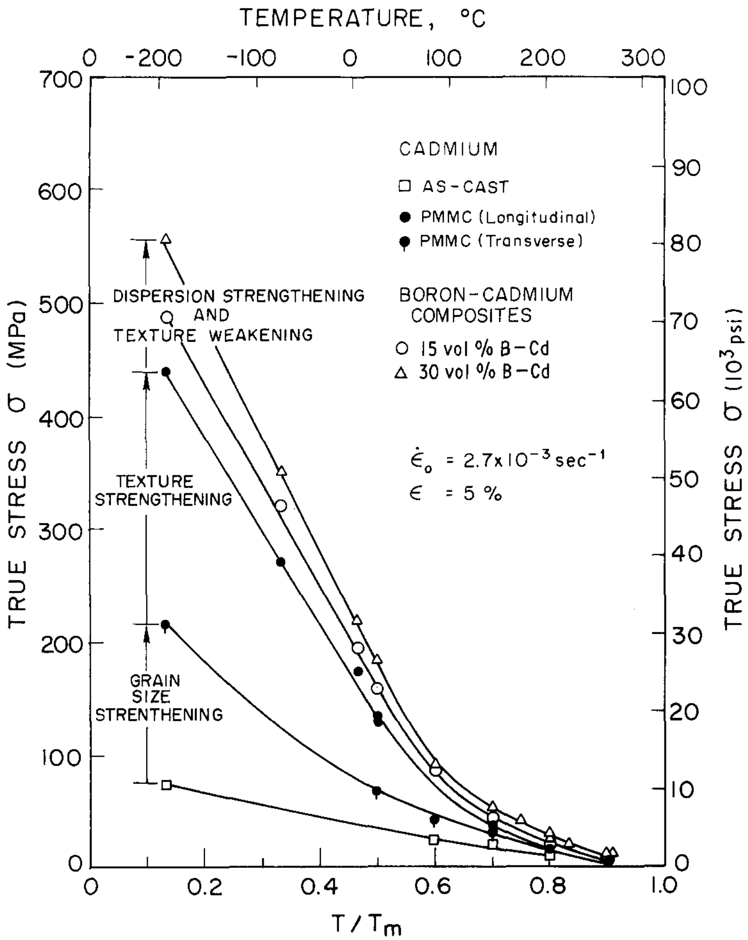

Figure 3 Influence of temperature on the flow stress of as-cast cadmium, powder metallurgy processed cadmium and cadmium–baron particulate composites.

dicated schematically in Fig. 5, was developed during extrusion of the fully processed powder metallurgy cadmium and this led to significant mechanical anisotropy. Thus, in order to determine the true grain size effect on strength of cadmium, it was necessary to consider any differences in texture created by processing. A Hall–Petch analysis of all readily available cadmium data [9, 10] is shown* in Fig. 5. These data are all for -196° C ($0.13T_m$), a temperature chosen for comparison because strain-rate does not influence the flow stress appreciably at such low temperatures and different strain-rates were used by each investigator. Data in the grain size range 30 to 1250 μm correlate very well on one straight line. We assume that these data refer to non-textured polycrystalline cadmium and have drawn a least squares best line to the data (Tegart [9] indicated that he had no texture in his samples whereas Riseborough and Teghtsoonian [10] did not report the amount of texturing in their samples). The flow stress for transverse samples of our powder metallurgy cadmium fits in quite well with the other data; this is reasonable since the transverse samples deform more nearly like a random polycrystalline aggregate (a large fraction of the transverse compression sample can deform by basal slip). The flow stress for the longitudinal sample, however, is much greater than that predicted by the straight line relation given. This observation is a direct consequence of the small fraction of basal planes available for plastic flow in longitudinal samples, requiring other, less facile, slip modes to participate in the deformation process, e.g. pyramidal slip [11]. Similar observations of the effect of preferred orientation on grain size strengthening in magnesium were recorded by Wilson and Chapman [12].

* Mannan and Rodriguez [24] studied the strength of polycrystalline cadmium in the grain size range 25 to 80 μm. Their data did not correlate well with the other data analysed (the strengths reported by Mannan and Rodriguez at -196° C were about 50% lower than those reported by others and for this reason were not plotted in Fig. 5.

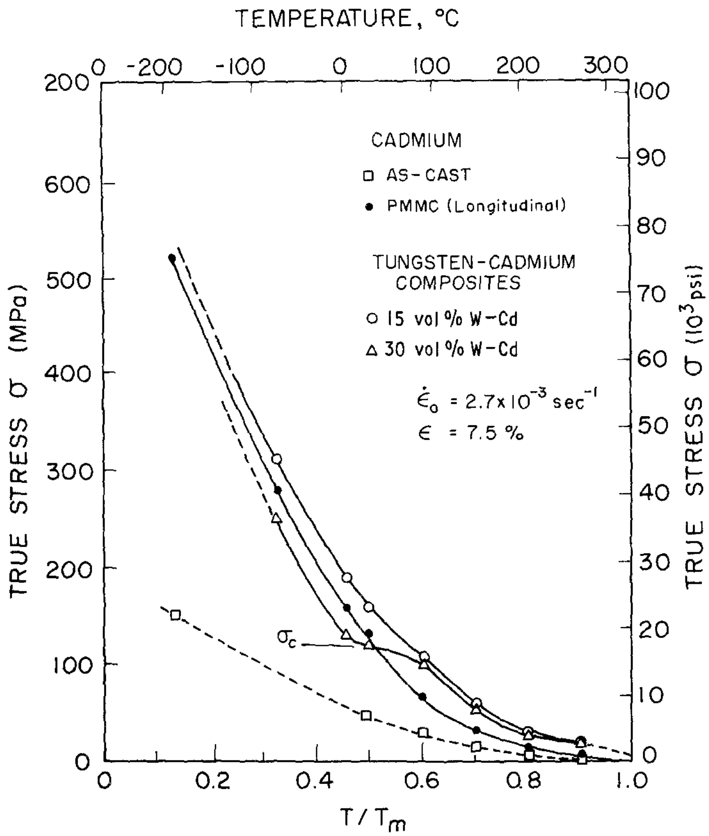

Figure 4 Influence of temperature on the flow stress of as-cast cadmium, powder metallurgy processed cadmium and cadium-tungsten particulate composites.

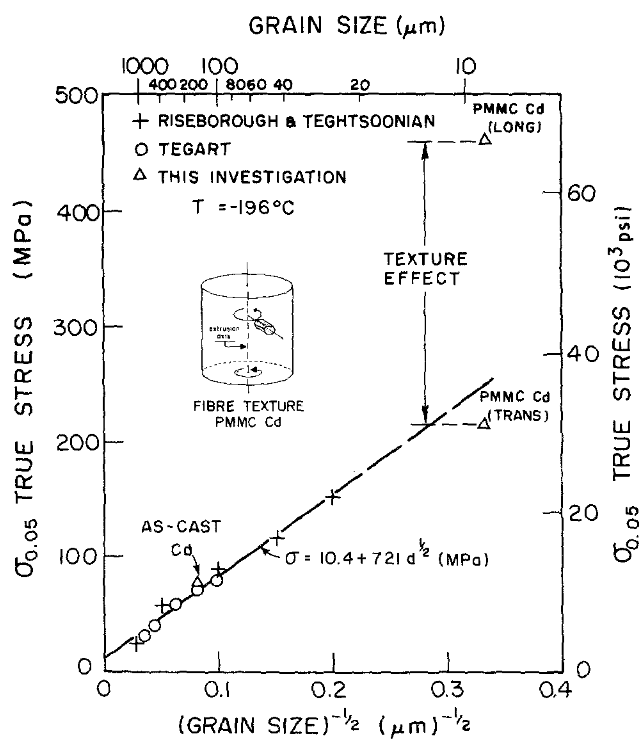

Figure 5 Influence of grain size on the flow stress of cadmium at −196° C.

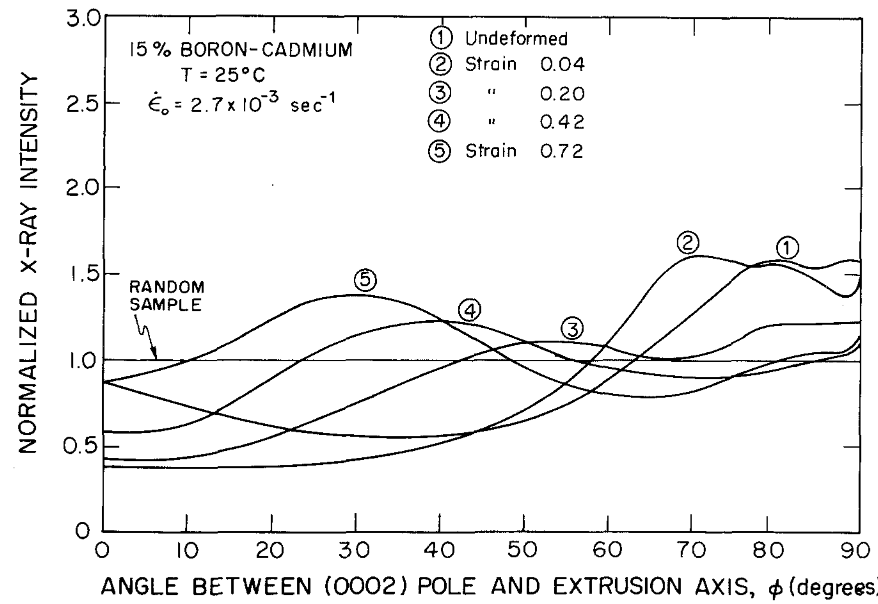

Figure 6 Influence of deformation at 25° C on the distribution of basal plane poles for the 15 vol% boron–cadmium composite.

We can now make an estimate of the factors contributing to the difference in low temperature strength of powder metallurgy cadmium (in the longitudinal direction) and the as-cast cadmium shown in Fig. 3. Using Fig. 5 as a guide, it would appear that grain-size refinement accounts for about 40% of the increase in strength and texture strengthening the remaining 60%, as indicated in Fig. 3.

5.2. Texture strengthening

The strong effect of preferred orientation was a pervasive influence in our study. We have already shown by the data of Fig. 5 that texture could be at least as significant as grain size in determining the compressive flow stress of cadmium. We also attribute the strain-softening effect shown in Fig. 2 (a prominent feature of deformation for all powder metallurgy alloys deformed at temperatures less than about 100° C) to changes in preferred orientation with strain. A similar conclusion was reached by Edwards *et al.* [13] who observed strain softening in powder metallurgy zinc. As mentioned earlier, our mechanical processing created a strong $\langle 1\,0\,\bar{1}\,0\rangle$ fibre texture in our materials. Fig. 6 shows the texture changes measured as a function of strain in a 15 vol% B–Cd composite deformed at the same strain-rate and temperature as used for the data of Fig. 2. It is obvious from Fig. 6 that a significant fraction of basal poles are reoriented by strain from positions near 70° with respect to the stress axis (line for $\epsilon = 0.04$) to positions near 30° (line for $\epsilon = 0.72$). Recognizing that basal glide is the preferred slip system for cadmium over a wide range of temperature [14], we can make a simple Schmid law calculation to estimate how the observed changes in texture could affect the uniaxial compressive stress needed to maintain basal glide. The stress to maintain basal slip in a grain of orientation ϕ_i is normally given by the Schmid law $\sigma_i = \tau_0/\cos\lambda_i \cos\phi_i$ where τ_0 is the resolved shear stress for slip, ϕ_i is the angle between the stress axis and the glide plane pole, and λ_i is the angle between the glide direction and the stress axis. This angle λ is related to ϕ and to η, the angle between the $\langle 1\,1\,\bar{2}\,0\rangle$ slip direction and the direction in the basal plane that is coplanar with the stress axis (fibre axis) and the basal pole by the expression $[\cos\lambda = \cos(90-\phi)\cdot\cos\eta]$ so that the expression for flow stress attributable to basal slip can be rewritten as:

$$\sigma_i = \frac{\tau_0}{\cos\phi\cdot\cos(90-\phi)\cdot\cos\eta} = \frac{2\tau_0}{\sin 2\phi\cdot\cos\eta} \qquad (1)$$

The angle η in our initial $\langle 1 0 \bar{1} 0\rangle$ fibre-textured cadmium is ideally 30° and will not change appreciably with deformation. Accordingly, Equation 1 can be simplified for an average $\eta_i = 30°$ as

$$\sigma_i = \frac{2.31\tau_0}{\sin 2\phi_i}. \qquad (2)$$

Returning now to the actual texture data of Fig. 6, if all grains were initially at an orientation of $\phi = 70°$, and were altered by strain to an orientation of $\phi = 30°$, the fractional change in flow stress observed should be that obtained from Equation 2, namely, $\sigma_2/\sigma_1 = \sin 140°/\sin 60° = 0.74$. The actual fractional change in flow stress observed for the 15 vol% B–Cd composite (see Fig. 2) was $\sigma_2/\sigma_1 = 0.62$ ($\epsilon_1 = 0.04$ and $\epsilon_2 = 0.72$). These calculations indicate that the magnitude of the change in flow stress agrees quite well with the observed change in texture. (A more quantitative attempt to correlate our texture measurements and mechanical test data is not appropriate, for the necessary analysis is very sensitive to small basal pole reorientations at high values of ϕ.) We thus conclude that associating that dispersion strengthening was observed for all texture changes observed is a reasonable interpretation of our results.

In addition to strain softening, another unusual characteristic of B–Cd composites compressed at a strain-rate of 10^{-3} sec^{-1} or greater, and temperatures of 25° C or less was the independence of flow stress at large strains on the volume fraction of boron particles introduced (Fig. 2). (Deformation at strain-rates lower or temperatures higher than the limits given above were more normal, in that dispersion strengthening was observed for all strains.) The same flow stress for all composites at large strains may indicate separation at particle/matrix interfaces, eliminating the influence of dispersion hardening. Other indirect evidence for this proposed occurrence is the lack of tensile ductility we observed for B–Cd composites. In contrast to W–Zn composites made by our process and previously reported [5, 6], cadmium-based composites were found to be less ductile at moderate strain-rates and ambient temperature than the matrix material prepared by the same process [15]. Tensile elongation data are summarized in Table III for B–Cd, W–Cd, and W–Zn composites. Elongations of only 1 to 4% were observed for the B–Cd composites whereas the W–Zn composites exhibited 30% elongation.

5.3. Particle strengthening

An empirical observation on particle strengthening of cadmium suggested the relation $\sigma \propto d^{-0.1}$ (d is the interparticle spacing), as shown in Fig. 7. Such a relation might, without additional investigation, be taken as complete characterization of the boron particle effect on the strengthening of cadmium at −196° C. Our earlier discussion, however, has shown the important influence of grain size and texture on the strength of cadmium. These two microstructural variables are a function of the boron content and must be taken into account to assess properly data of the type given in Fig. 7. For example, a study of the effect of boron particle additions on preferred orientation showed that an increase in the number of boron particles resulted in a weaker final $\langle 1 0 \bar{1} 0\rangle$ fibre texture. These data are plotted in Fig. 8, which indicates that a 3 vol% B–Cd composite is strongly textured, whereas a 30 vol% B–Cd composite, while still not random, is significantly less textured than composites containing less boron.

TABLE III Tensile properties of B–Cd, W–Cd and W–Zn composites at 25° C

Material		$\dot{\epsilon}_0$ (sec^{-1})	$\sigma_{max}(\epsilon = 0.01)$(MPa)	elongation (%)
PMMC–Cd		3×10^{-3}	102	22
Boron–cadmium (vol%)	3	3×10^{-3}	129	4.3
	15	3×10^{-3}	134	2.4
	30	3×10^{-3}	150	1.0
Tungsten–cadmium (vol%)	1.4	3×10^{-3}	119	12
	15	3×10^{-3}	156	2.0
	30	3×10^{-3}	112	1.5
PMMC–Zn		2×10^{-4}	168	7.0
W–Zn (vol%)	30	2×10^{-4}	83	30.0

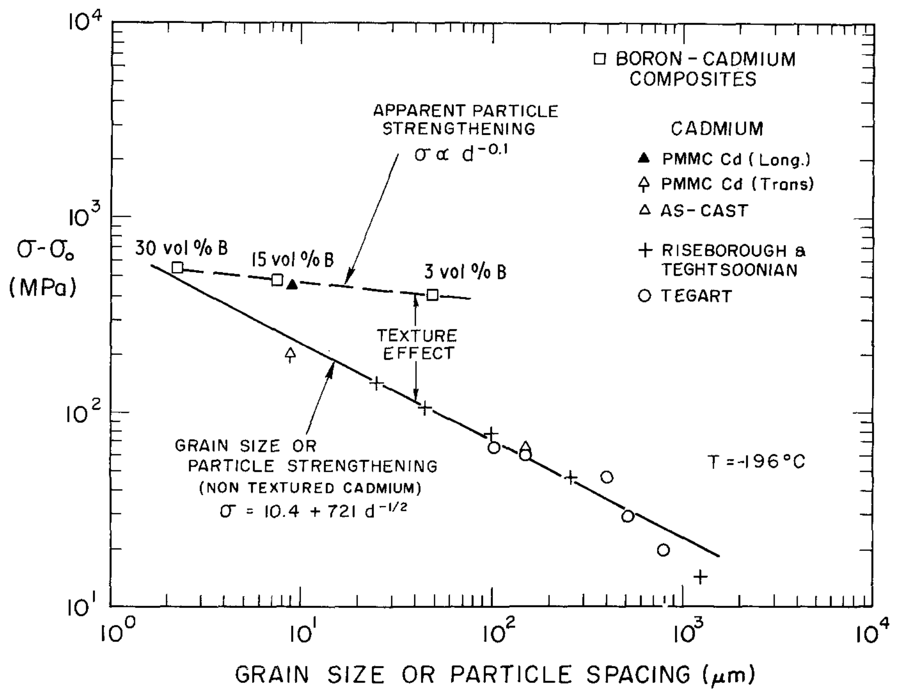

Figure 7 Influence of interparticle spacing on the flow stress of cadmium–boron particulate composites at −196° C. The grain-size strengthening curve of Fig. 4 is included for comparison (σ_0 = 10.4 MPa).

The strength of B–Cd particulate composites can be analysed by a Hall–Petch type relation following the ideas used by Liu and Gurland [16, 17]. Thus, in the expression

$$\sigma_F = \sigma_0 + k_y l^{-1/2}. \qquad (3)$$

l is the smallest microstructure feature in the material (grain size, subgrain size or particle spacing), σ_F is the flow stress at constant strain, and σ_0 and k_y are material constants. Following this approach, we have extended the range of the empirical relation determined in Fig. 5 for non-textured cadmium by replotting the data in Fig. 7 as flow stress less the friction stress, $\sigma - \sigma_0$, (at 5% strain and −196° C) against grain size or particle spacing (double log scale). The correlation suggested by Liu and Gurland [16, 17] adequately describes the boron particle strengthening effect in cadmium if variations in the extent of texturing are also considered. Thus, the 30 vol % B–Cd com-

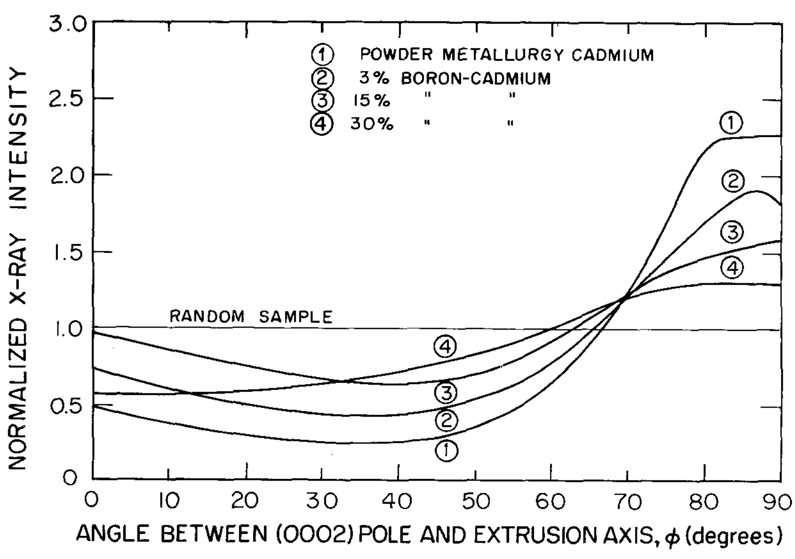

Figure 8 Influence of boron on the amount of texturing obtained in cadmium-boron particulate composites.

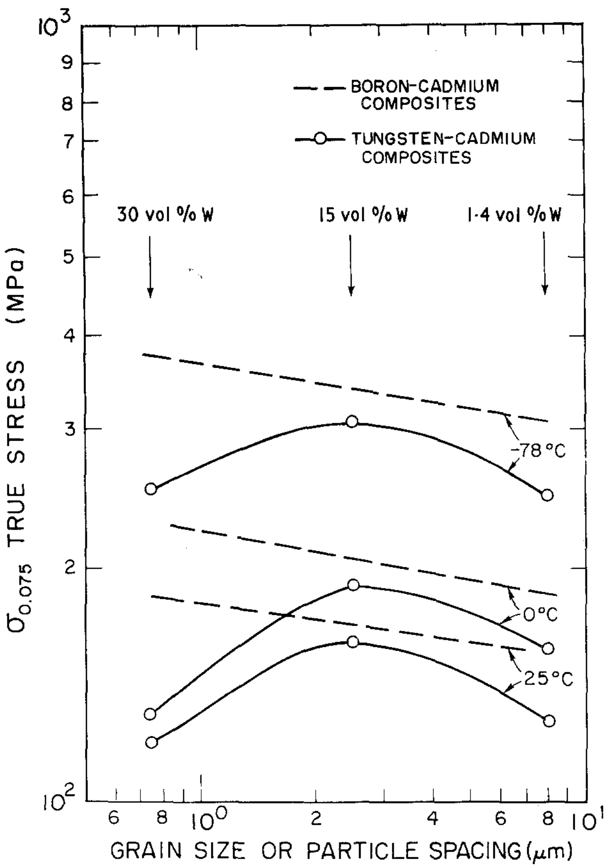

Figure 9 Influence of grain size or particle spacing (which ever is smallest) on the flow stress of Cd–B and Cd–W composites.

posite is very nearly as strong as that predicted by the proposed relation (given by the curve representing the strength behaviour of non-textured polycrystalline cadmium, Fig. 7). This is reasonable since the 30 vol% B–Cd composite has a very weak texture (Fig. 8). The 15 vol% B–Cd composite (where both interparticle spacing and grain size are equal to 7.5 μm, Table II) falls above the proposed relation; this increase in strength can be explained by the presence of a texture (Fig. 8). The 3 vol% B–Cd composite, even after correcting for the fact that its grain size (8 μm) is much finer than the interparticle spacing ($d = 49\ \mu$m) also lies above the proposed relation; this behaviour is similar to the 15 vol% B–Cd composite and the increased strength can also be attributed to the strong texture present in this composite.

The previous remarks concerning strengthening effects by grain refinement, preferred oreintation and dispersed particles observed in B–Cd composites apply equally well to W–Cd composites. The major exception was found to be associated with the dispersion-strengthening effect of tungsten for volume fractions greater than 0.15. Fig. 9 indicates that while tungsten additions up to 15 vol% gave dispersed particle effects quite comparable to those found for boron additions, fabrication of a 30 vol% W–Cd composite resulted in a weaker material. Since this effect persists at temperatures equal to $0.5T_m$ and at low strains, it is not thought to be associated with particle/matrix separation. A similar result has been observed in W–Zn and Al_2O_3–Zn composites, where there is very clear evidence that localized material failure does not occur [3–6, 18, 19]. In zinc-based composites, dispersion weakening and associated mechanical effects have been successfully modelled on the premise that primary sources of dislocations in these fine-grained materials at certain temperatures and strain-rates are the dispersed particles themselves [20]. Fig. 4 plots flow stress versus temperature at 5% strain and $\dot{\epsilon}_0 = 2.7 \times 10^{-3}\ \text{sec}^{-1}$ for as-cast and powder metallurgy cadmium and for two W–Cd composites. It is obvious that the anomaly of the dispersion weakened 30 vol% W–Cd composite persists over the entire temperature range, but that an inflection occurs at $\sigma_c = 120$ MPa, above which the dispersion weakening is most pronounced. A critical stress such as σ_c was interpreted by Edwards *et al.* [20] as the threshold stress above which dispersed particles would operate as sources for mobile dislocations. A threshold stress $\sigma_c = 120\,\text{MPa}$ for cadmium containing $0.6\,\mu\text{m}$ tungsten particles agrees quite well with both experimental [21] and calculated [22, 23] values of σ_c. It is, however, not clear to us why a threshold stress is observed for the 30 vol% W–Cd composite but not for the high volume fraction B–Cd composite. It may well relate to the shape and size distribution of B and W particles in cadmium.

5. Conclusions

Marked strengthening of cadmium by additions of small (0.6 to $3\,\mu\text{m}$) boron or tungsten particles by a powder metallurgy process can be attributed to significant grain size and texture strengthening effects as well as to dispersion strengthening effects. Both grain size and boron dispersion strengthening compare reasonably with the work of other researchers [9, 10,16,17]. A dispersion weakening anomaly in W–Cd composites is compatible with similar results in zinc-based composites [5, 19, 20] and can probably be associated with generation of mobile dislocations at particle–matrix interfaces.

6. Acknowledgements

The authors gratefully acknowledge the financial support of the Office of Naval Research under Project N00014–C–0062, and the Naval Postgraduate School Foundation Research Grant Program. We wish to thank especially Drs W. G. Rauch and B. A. MacDonald for their encouragement and many helpful discussions.

References

1. H. ETHERINGTON, ed., "Nuclear Engr. Handbook", (McGraw Hill 1958) pp. 13–124.
2. R. W. DAYTON, "Reactor Handbook," 2nd Edn. (Interscience, New York, 1960) pp. 777–809.
3. W. H. McCARTHY, Ph.D. Dissertation, Stanford Univeristy (1966).
4. W. H. McCARTHY, J. C. SHYNE and O. D. SHERBY, *Trans. ASM* **62** (1969) 117.
5. G. R. EDWARDS, Ph.D. Dissertation, Stanford University (1971).
6. G. R. EDWARDS and O. D. SHERBY, *Int. J. Powder Met.* **7** (1971) 21.
7. S. CHANDRASEKHAR, *Rev. Mod. Phys.* **15** (1943) 1.
8. M. F. ASHBY and R. EBELING, *Trans. Met. Soc. AIME* **236** (1966) 1396.
9. W. J. Mcg. TEGART, *J. Inst. Metals* **91** (1962–63) 99.
10. N. R. RISEBOROUGH and E. TEGHTSOONIAN, *Canad. J. Phys.* **45** (1967) 591.
11. N. S. STOLOFF and F. GENSAMER, *Trans. Met. Soc. AIME* **224** (1962) 732.
12. D. V. WILSON and J. A. CHAPMAN, *Phil. Mag.* **8** (1963) 1543.
13. G. R. EDWARDS, J. C. SHYNE and O. D. SHERBY, *Met. Trans.* **2** (1971) 2955.
14. P. G. PARTRIDGE, *Met. Rev.* **12** (1967) 169.
15. S. HSU, Ph.D. Dissertation, Stanford University (1972).
16. C. T. LIU and J. GURLAND, *Trans. ASM* **61** (1968) 156.
17. J. GURLAND, Proceedings, International Conference on the Strength of Metals and Alloys, Vol. 2 (American Society for Metals, 1970) p. 621.
18. T. R. McNELLEY, Ph.D. Dissertion, Stanford Univeristy (1973).
19. T. R. McNELLEY, G. R. EDWARDS, D. FRANCOIS, W. H. McCARTHY, J. C. SHYNE and O. D. SHERBY, *Met. Trans.* **3** (1971) 1316.
20. G. R. EDWARDS, T. R. McNELLEY and O. D. SHERBY, *Phil. Mag.* **32** (1975) 1245.
21. M. F. ASHBY, S. H. GELLES and L. E. TANNER, *ibid* **19** (1969) 757.
22. M. F. ASHBY and L. JOHNSON, *ibid* **20** (1970) 1009.
23. L. M. BROWN, G. R. WOOLHOUSE and U. VALDRE, *ibid* **17** (1968) 781.
24. S. L. MANNAN and P. RODRIGUEZ, *Acta Met.* **23** (1975) 221.

Received 9 March and accepted 2 April 1976.